Article

Molecular Characterization of Nonvolatile Fractions of Algerian Petroleum with High-Resolution Mass Spectrometry

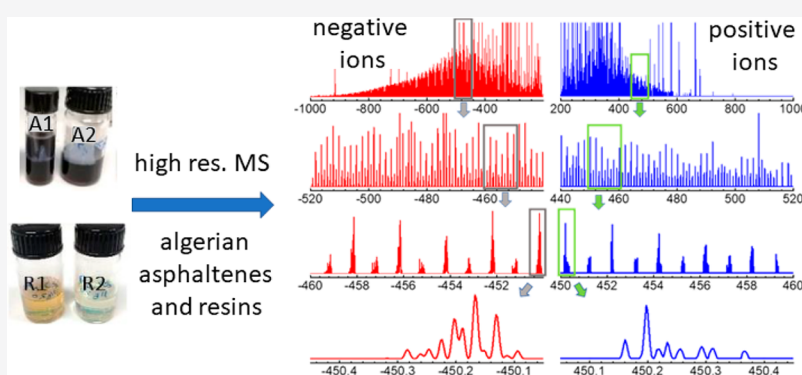Fatima Saad, Boumedienne Bounaceur, Mortada Daaou,* Juan Ramón Avilés-Moreno, and Bruno Martínez-Haya

ACCESS | Metrics & More | Article Recommendations

ABSTRACT: Algerian crude oil displays a marked propensity for asphaltene precipitation, leading to solid deposits during extraction, transportation, and storage. The relationship between precipitation and chemical composition is unclear; in fact, Algerian crude oil actually features a low asphaltene concentration, despite its relatively large rate of deposit formation. The rationalization of the precipitation process and its remediation should benefit from a molecular characterization of the crude oil. In this study, two unstable asphaltene fractions (A1 and A2) from two different deposits, and two resin crude oil fractions (R1 and R2) from the Hassi-Messaoud Algerian field have been characterized at the molecular level by means of high-resolution mass spectrometry with an Atmospheric Pressure Chemical Ionization (APCI) source. Positively and negatively charged compounds with molecular weights 200−1200 m/z were detected. Several thousand molecular stoichiometries were identified and classified for each sample, in terms of heteroatom content and aromaticity, searching for trends characteristic of the two asphaltenes and of the associated resins. The A2 asphaltene, from a downstream storage tank, displays a higher aromaticity and O-heteroatom content, which correlates with an enhanced aggregation propensity, in comparison to the A1 fraction, collected at the well bore. The resin fractions are found to be abundant in aliphatic hydrocarbons and heteroatomic compounds of moderate aromaticity. The more polar resin fraction, R2, is enriched in N-containing species, with respect to the less polar resin fraction R1, which correlates with the stabilizing function observed in previous works. The results stress the view of crude oil fractions as complex mixtures, rather than in terms of average prototypical compounds, when facing the understanding of asphaltene deposition conditions.

INTRODUCTION

Asphaltenes are an extremely complex mixture of polyaromatic compounds, encompassing the heaviest and most polar fraction of crude oil.[1] The molecular complexity of asphaltenes is a direct consequence of their phenomenological definition, in terms of solubility properties in aromatic solvents (toluene) versus light paraffinic solvents (e.g., *n*-heptane or *n*-hexane). There is solid experimental evidence supporting the theory that asphaltenes plausibly extend over molecular weights within the range of 200−2000 g/mol, and that they consist of polyaromatic species with varying abundances of condensed island-like and cross-linked archipelago-like structures and of heteroatom content (primarily oxygen, nitrogen, and sulfur).[2−6] In addition, trace amounts of metals such as Ni, Fe,

and V are present in asphaltenes, potentially contributing to their physicochemical properties.[7]

The extensive efforts devoted in the past decades to the elucidation of the molecular nature of asphaltenes and their related colloidal behavior relies on the enormous problems that they cause during the production, transportation, storage, and

refining of crude oil. Asphaltenes are prone to precipitation and formation of solid deposits, eventually leading to plugging of pipelines and even wellbores, with significant costs related to remediation and loss of production. Consequently, oil companies invest significant budgets in chemicals that prevent asphaltene deposition.[8] For instance, in the Hassi−Messaoud fields, more than 80 wt % of the asphaltenes in the crude oil eventually become incorporated into deposits in the tubing, which demand frequent washing treatments and injection of solvents and dispersants.[9,10]

The mechanisms leading to asphaltene deposit formation are complex and are not fully understood to date. Pressure, temperature, and compositional changes in the oil may have nontrivial effects on asphaltene precipitation.[11] The molecular structure and the interactions of asphaltenes with other constituents of crude oil are considered important sources of modulation of their stability or precipitation. It has been suggested that asphaltenes with a higher polarity (higher heteroatom content) have a tendency to be more unstable, with respect to aggregation.[12−20] Resin molecules are considered stabilizing agents that bind efficiently to asphaltenes, presumably preventing the growth of incipient aggregates.[21−34] The presence of polar heteroatom groups and of small aromatic moieties in resins appears to pose the largest deterring effects on asphaltene precipitation.[35−38]

Therefore, the molecular characterization of asphaltenes and resins seems to be key to rationalizing aggregation and flocculation processes in crude oils. High-resolution mass spectrometry stands out among other analytical techniques, because of its ability to define the elemental composition and structure of crude oil constituents.[1] Molecular stoichiometries (e.g., $C_cH_hN_nO_oS_s$) are determined from the accurate measurement of exact masses. Structural information may be inferred from mass sequences and trends associated with heteroatom content, assisted by fragmentative MS/MS techniques.[2−5] The consolidation of commercial Fourier transform−ion cyclotron resonance (FT-ICR), orbitrap and time-of-flight (TOF) mass analyzers, in combination with a range of ionization techniques, such as electrospray ionization (ESI), atmospheric pressure photoionization (APPI), atmospheric pressure chemical ionization (APCI), or laser desorption/ionization (LDI), has largely contributed to the recent advances in petroleum science.[1−5,39−51] Among them, orbitrap mass spectrometry is currently being considered as a cost-effective benchtop high-resolution technique and it is finding increasing application in the field of petroleomics.[39,43−46]

In this paper, APCI-orbitrap mass spectrometry has been employed to characterize resin fractions and asphaltene deposits of Algerian crude oil from the Hassi-Messaoud fields. This crude oil constitutes a paradigmatic case of a large precipitation tendency, in apparent contrast with a comparably poor asphaltene content, of <1 wt %.[9] Several studies have described the physicochemical behavior of Algerian crude oils and have evaluated their response to flocculants and emulsion stabilizers.[34,52−56] Despite such rich literature around the precipitation problem, few previous studies have addressed the detailed characterization of nonvolatile fractions (i.e., asphaltenes and resins) of Algerian crude oils at a molecular level.[52,57,58] A first incursion of our groups into the composition of Algerian asphaltenes, based on LDI mass spectrometry in combination with spectroscopic methods (FT-IR and NMR), showed that the structural properties of asphaltenes present in petroleum may vary significantly during

the different stages of extraction, treatment, transportation and storage.[19,59] A detailed correlation of crude oil deposits formed during those processes with compositional and structural changes (aromaticity, polarity and heteroatom content, etc.) was pending, because of the limited mass resolution of the TOF mass spectrometer employed.

This study focuses on the analysis of two differentiated crude oil deposits: one that is formed at the wellbore, plausibly associated with the gas-enhanced oil recovery employed in the field, and a second one that is formed downstream after extensive treatment and transportation of the oil. Profound differences are found between the composition of the asphaltenes extracted from the two deposits, which correlate with their aggregation propensity. The resins were characterized based on their potential role as stabilizers against asphaltene precipitation.

Consistent with previous high-resolution mass spectrometry investigations, the present results stress the importance of understanding crude oil fractions as complex mixtures, polydispersed in composition and structure, rather than viewing them in terms of average prototypical compounds.

2. MATERIALS AND METHODS

Crude oil samples and two asphaltene deposits from the Algerian Hassi-Messaoud petroleum field were supplied by the Sonatrach Company. General characteristics of Hassi-Messaoud petroleum are summarized in Table 1.

Table 1. General Physical Characteristics of the Crude Oil from the Hassi−Messaoud Well[a]

| parameter	value
gravity	45° API
viscosity at 40 °C	2.23 cP
total acidity	0.96 mg KOH/g
resin content	24.5% (w/w)
asphaltene content	0.70 (w/w)

[a]Data taken from ref 20.

The first deposit (DP1) was formed at the wellbore during enhanced oil recovery based on the injection of a gas mixture of C1−C5 hydrocarbons with 10% CO_2. The second deposit of the same oil (DP2) was formed at the entrance of a downstream storage tank, to which the crude oil was transported after degassing and treatment for the removal of salts and water.

Toluene (99% purity), CS_2 (99% purity), acetone, methylene chloride (99% purity), and dithranol (MALDI matrix, 99% purity) were supplied by Sigma−Aldrich, while n-hexane and n-heptane (98% purity) were purchased from Biochem Chemicals.

2.1. Extraction of Asphaltene and Resin Fractions. The extraction of the resin fractions was performed on crude oil collected at the wellbore, according to the ASTM D-2007 guidelines[60] outlined in Figure 1. As described in detail elsewhere,[34] the protocol fractionates deasphalted oil into saturates, aromatics, and two resin fractions, namely, a low polarity resin fraction and a high polarity resin fraction, which will be referred to as R1 and R2, respectively.

Asphaltenes from deposit DP1 were extracted with either n-heptane (C_7-A1) or n-hexane (A1) as flocculant. Asphaltenes from deposit DP2 (A2) were extracted with n-hexane. In all cases, the flocculant was added in an excess of 40:1 (cm^3/g) ratio to the crude oil deposit. The mixture was stirred for 24 h in darkness at ambient temperature, and subsequently allowed to precipitate for additional 24 h. Finally, the precipitated asphaltenes were retained in filter paper with a pore diameter of 45 μm, and then dissolved in toluene. After evaporation of the solvent, asphaltenes were washed several times with fresh flocculant, until a visually clean supernatant was obtained. The
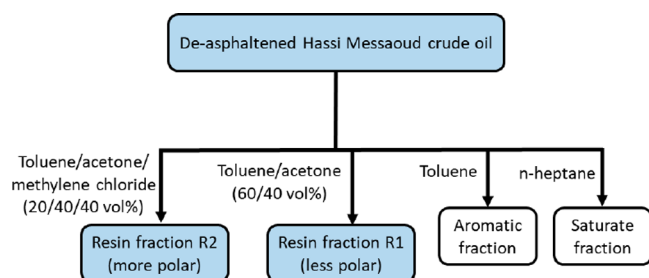
Figure 1. Schematic layout of the protocol employed for the extraction of resin fractions.

extraction procedure resulted in recovery yields of 88 wt % and 85 wt % for the *n*-hexane asphaltenes A1 and A2, respectively, and of 60 wt % for the *n*-heptane asphaltene C_7-A1.

2.2. Elemental Analysis of Asphaltene and Resin Fractions. Elemental composition (carbon, hydrogen, nitrogen, and sulfur) of the asphaltene and resin fractions were determined with a CHNS TruSpec Micro (LECO) elemental analyzer. Sulfur content was confirmed by inductively coupled plasma (optical ICP) quantification. The results of the elemental analysis of the A1, C_7-A1, A2, R1, and R2 fractions are listed in Table 2, and they are discussed in Section 3.1.

Table 2. C, H, N, and S Composition (Weight Percentage), and Associated H/C Atomic Ratio of the Asphaltene and Resins Extracts Included in This Investigation

sample	Composition (Weight Percentage)					H/C
	C	H	N	S	O[a]	
A1	87.7	7.7	0.86	0.42	3.3	1.05
C_7-A1	88.5	7.9	0.86	0.40	2.5	1.07
A2	79.5	6.0	0.14	0.41	13.9	0.90
R1	84.3	12.6	0.10	0.85	2.1	1.79
R2	77.6	10.9	0.35	1.40	9.7	1.68

[a]Oxygen evaluated from the mass balance.

Given the apparently anomalous O content of asphaltene A2, we analyzed all samples in an independent facility in Seville, which delivered statistically coincident results.

2.3. Aggregation Onsets of the Asphaltene Fractions. To compare the stability of the asphaltene fractions, the aggregation onset point (AGO) and the precipitate content (wt %) of each asphaltene fraction were determined, using conventional methods based on ultraviolet–visible (UV-vis) spectrophotometry and gravimetry.[19] In particular, absorbance at 750 nm was monitored as flocculant was added to toluene solutions of the asphaltenes, searching for light scattering effects associated with precipitated asphaltene particles.

2.4. APCI-Orbitrap Mass Spectrometry. The molecular analysis of asphaltenes and resins was conducted using a Q-Exactive Focus Hybrid Quadrupole-Orbitrap Mass Spectrometer (Thermo-Fisher) that was equipped with an APCI ion source. APCI is based on the nebulization of the sample and the generation of a corona discharge, yielding a chain of charge/proton transfer reactions, eventually ionizing the analytes.[61] It is an efficient ionization technique for thermally stable molecular species of moderate size (up to 2000 amu) with medium to high polarity.[62] In the present experiments, positive and negative ion mass spectra were acquired in full scan mode over the absolute mass range 200–1200 *m/z*, at a nominal resolving power of $M/\Delta M = 60\,000$ at *m/z* 300. Hence, the full width at half-maximum (fwhm) values of the individual peaks in the mass spectra ranged from 0.002 at *m/z* 300 to 0.007 at *m/z* 800, and the mass accuracy was of 5 ppm, as tested with different polyaromatic hydrocarbon calibration standards. The samples to be analyzed (asphaltenes or resins) were dissolved in carbon disulfide (CS_2) at 1 mg mL⁻¹ concentration and then sonicated for 20 min. Using CS_2 as a solvent provided stronger signals than other organic solvents, e.g.,

toluene, because of a more efficient sample ionization in the APCI source, which is consistent with previous works.[63−65] The solutions were directly infused into the APCI source at a flow rate of 50 μL min⁻¹. The discharge current was set at 5 μA in all measurements. The temperature of the inlet capillary in the ionization source was maintained at 275 °C, while the temperature of the APCI vaporizer was adjusted for maximum ion signal to 300 and 450 °C in the positive and negative ion modes, respectively. Increasing the temperature for the positive-ion mode measurements deteriorated the signal without an appreciable trend of detection of a broader range of chemical species. Test measurements with lower asphaltene concentrations, down to 0.2 mg mL⁻¹, did not yield evidence for changes in the ion distribution, because of potential signal suppression induced by aggregation effects.[2]

2.5. LDI-TOF Mass Spectrometry. Laser desorption ionization mass spectra with time-of-flight mass discrimination (LDI-TOF) of the asphaltenes and resins were collected in a Bruker-Daltonics UltrafleXtreme mass spectrometer, equipped with a 355 nm Nd:YAG laser. The laser pulse energy was set at 20% above the detection threshold of each sample (∼5 μJ), and 2500 laser shots were accumulated to produce each spectrum at a laser firing rate of 500 shots s⁻¹. Positive-ion spectra were recorded in linear time-of-flight mode, leading to a mass resolution of $M/\Delta M = 6000$ at *m/z* 300. The instrument was calibrated using external polyaromatic and poly-dispersed polymer standards with masses of 300−1500 *m/z*.

The conventional dried-droplet method was employed to spot 1 μL of 1 mg mL⁻¹ sample solution on the stainless-steel sample plate; the solvent was then allowed to dry in air for several minutes. Using CS_2 or toluene led to LDI mass spectra or similar quality. In a series of test measurements aimed at reducing supramolecular aggregation effects in the mass spectrometer,[50] an excess of dithranol was added to the sample solutions to dilute the asphaltene and resin samples in the final precipitate. However, the recorded spectra did not show any significant effects from the addition of dithranol. While dithranol, a common MALDI matrix, may as well assist the ionization of the sample, this is uncertain in the present case, since a large fraction of the asphaltene and resin constituents efficiently absorb the laser light and similarly activate the desorption/ionization process.

2.6. Data Analysis. The peaks observed in the APCI-orbitrap mass spectra were assigned to molecular stoichiometries of the form $C_cH_hN_nO_oS_s$, based on the recorded exact masses. Each peak in the spectrum was assigned to the stoichiometry that provided the best concordance with the experimental mass. The mass resolution and tolerance (5 ppm) of our mass spectrometer are at the limit required for the identification of sulfur, because of the small difference of ca. 0.003 Da between the masses of C_3 and SH_4. Consequently, sulfur was introduced in the fitting procedure only if no satisfactory mass match was otherwise obtained. The number of peaks assigned to compounds with one S atom was <2% in all cases and corresponded to compounds within the high-resolution end of the spectrometer (*m/z* < 400).

The molecular species thus identified were then classified in terms of their heteroatom content and aromaticity, as described by different parameters, including double-bond equivalents (DBEs) and Kendrick mass defects (KMDs). The DBE is defined according to the "nitrogen rule":

$$\text{DBE} = n_C - \frac{n_H}{2} + \frac{n_N}{2} + 1$$

where n_C, n_H, and n_N denote the number of carbon, hydrogen, and nitrogen atoms in the molecule, respectively.[66,67] The Kendrick mass scale assigns a full mass of 14 amu to $^{12}CH_2$, and it is consequently related to the IUPAC ^{12}C mass scale through a factor of 14.00000/14.01565.[68,69] The Kendrick scale becomes particularly comprehensive when the analytes can be sorted out into families sharing heteroatom content and differing in the length of aliphatic chains, since the net incorporation or removal of CH_2 groups does not alter the Kendrick mass defect. Conversely, the incorporation of ring units to condensed polyaromatic structures may be achieved with a change

in mass equivalent to C_2, C_3H, or C_4H_2, involving changes in KMD of 0.027, 0.033, or 0.040 amu, respectively.

3. RESULTS

3.1. Elemental Analysis. The results of the C, H, N, S elemental analysis of the asphaltene and resin fractions are summarized in Table 2. The *n*-hexane (A1) and *n*-heptane (C_7-A1) asphaltenes from deposit DP1 show a similar percentage weight of C (~88%), while A1 displays a roughly 20% greater heteroatom content (4.5% vs 3.75%). These values differ significantly from those observed for the *n*-hexane asphaltene from deposit DP2 (A2), which displays a remarkably low percentage weight of C (79.5%), which is indicative of a high heteroatom content. The elemental analysis yields similar values for sulfur in all of the asphaltenes, and a smaller abundance of nitrogen in asphaltene A2 vs asphaltene A1. Hence, a large oxygen content in asphaltene A2 (~14%) emerges as the most plausible explanation for the small carbon weight. Unfortunately, we could not perform direct analysis of the oxygen content of our samples with the techniques at hand; the values in Table 2 are inferred from mass balance. While such a high oxygen content may seem unusual, similar values, ranging within 10%−14%, have been reported in previous analyses of downstream deposits of crude oil from different wells within the Hassi−Messaoud fields.[19,59] The stage of processing or aging mechanism responsible for the oxygenation of the crude oil is under discussion with the engineers of the Sonatrach Company and will be the topic of future research.

The polar resin fraction, R2, consistently displays a greater heteroatom content than its less-polar counterpart resin R1 (~12 wt % vs 3 wt %, respectively). Although the abundance of all heteroatoms increases in resin R2 vs resin R1, the main contribution is related to the oxygen content. Moreover, the net H/C values suggest that the A2 and R2 fraction exhibit higher aromaticity than their A1 and R1 counterparts.[70]

3.2. Aggregation Onsets. The stability of the asphaltenes was assessed in terms of their precipitation propensity in toluene solution (5 mg/mL) with *n*-hexane as a flocculant. Figure 2 shows the change in absorbance at 750 nm, recorded as a function of added volume of *n*-hexane. The absorbance initially decreases because of dilution of the asphaltenes; the threshold for aggregation is detected as a sudden increase of the apparent absorbance associated with light dispersion, which defines the aggregation onset (AGO).[19]
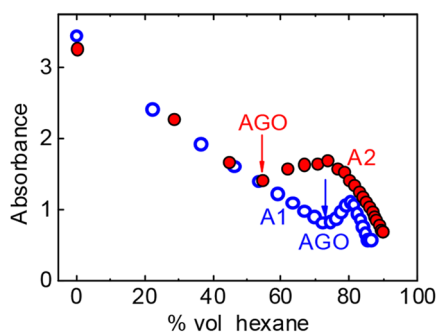
Figure 2. Determination of the aggregation onset (AGO) of asphaltenes A1 and A2 in 5 mg/mL toluene solution (open blue and solid red symbols, respectively). The absorbance at 750 nm is monitored as an increasing volume of hexane is added to the toluene solution, to induce precipitation.

The results indicate that the A2 asphaltenes are less stable (AGO = 55 vol % of *n*-hexane; precipitate content = 52 wt %) than the A1 asphaltenes (AGO = 72 vol % of *n*-hexane; precipitate content = 20 wt %). Note that the higher oxygen content of the A2 asphaltene correlates with a higher propensity to flocculate, in comparison to the A1 asphaltenes. This indicates that degradation/aging of the Hassi−Messaoud asphaltenes due to processing and storage has a particularly large effect on the formation of deposits.

3.3. APCI-Orbitrap Mass Spectra. APCI-orbitrap mass spectra were recorded for the asphaltene and resin samples in positive and negative ion mode, with the aim of monitoring the greatest diversity of molecular species possible and of highlighting the relative abundances of acidic (deprotonated negative ions) and basic (protonated positive ions) polar species. Recall that crude oil extracts are particularly complex materials, so information about their compositional landscape, provided by any instrumental technique, will be biased according to analytical responses. In the case of mass spectrometry, ionization efficiencies may vary over many orders of magnitude for different chemical families, depending on the type of source employed. For instance, electrospray ionization is most sensitive to polars and laser desorption ionization to polyaromatic species, with little efficiency for aliphatic compounds. The APCI source presently employed is most suitable for species of moderate size with medium to high polarity.[62] Consequently, it has been shown that multiple separation stages of crude oil extracts may be required to have access to compounds with low relative analytical responses.[3,41] This work constitutes a first incursion into the application of high-resolution mass spectrometry to the characterization of Algerian crude oils. Future studies will explore the implementation of specific sample pretreatment and differential precipitation procedures to further subfractionate the asphaltene and resin extracts.

The APCI-orbitrap mass spectra for the asphaltene A1 and A2, and resin R1 and R2 samples are displayed in Figure 3 at different degrees of magnification, to illustrate characteristic trends related to (i) the mass spread of the analytes over the 200−1000 *m/z* range; (ii) peak recurrences with 14 or 2 Da periodicities, related to the incorporation or removal of CH_2 groups (length of side chains) or pairs of H atoms (number of double bonds), respectively; and (iii) the ensemble of peaks that are observed within any given nominal mass. Figures 4 and 5 provide examples of peak assignments, further illustrating the diversity of heteroatom classes observed in the crude oil extracts.

In general terms, the negative ions reach greater molecular weights than the positive ions. While the negative-ion spectra display analytes up to 1000 *m/z*, the positive-ion spectra have comparably weak signals above 800 *m/z*. This is plausibly related to the higher sensitivity of APCI for polar compounds. In addition, the negative-ion mass spectra has a tendency to detect a greater variety of molecular stoichiometries within each nominal mass (above 10 in most cases). Figure 4 lays out an illustrative assignment of the chemical classes (C_xH_y, O_x, N_y, N_yO_x) observed for each material in positive- and negative-ion modes. The positive-ion spectra incorporate a larger fraction of native hydrocarbons with C_xH_y stoichiometries, while the negative-ion spectra capture compounds with higher heteroatom content. Measuring both ion polarities is key to exposing the different composition of the four samples through specific features and trends in the mass spectra. Note, for
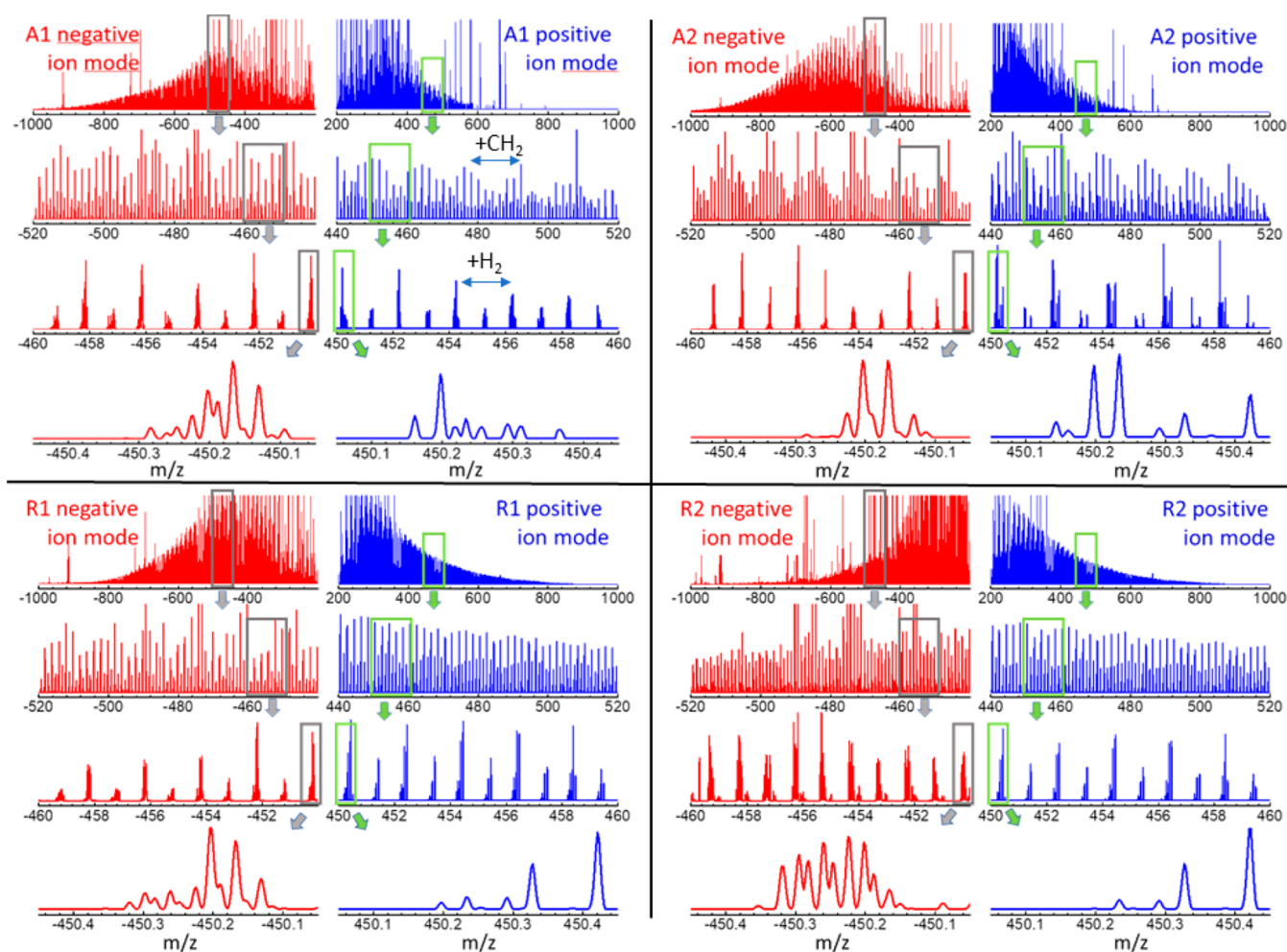
Figure 3. APCI-orbitrap spectra in negative- and positive-ion modes (red and blue traces, respectively), recorded for the asphaltene (A1, A2) and resin (R1, R2) extracts from Algerian crude oil. The complexity of the spectra is illustrated at different levels of amplification of the mass range. See Figures 4 and 5 for illustrative assignments of the observed peaks to molecular stoichiometries.

instance, that the two resin fractions produce similar mass spectra in positive-ion mode but display significantly different ensembles of chemical compounds in negative-ion mode. Conversely, the positive-ion spectra allow discerning asphaltenes from resins more neatly than, for instance, the negative-ion spectra of asphaltene A2 and resin R1. The higher degree of aromaticity of the asphaltenes over the resins is apparent from the DBEs of the molecular species observed within the 450−451 Da spectral window used for illustration. The overall DBE distributions are discussed below.

Figure 3 highlights collective peak position and intensity trends in the recorded mass spectra that are related to changes in length of the side chains and in the number of double bonds. Figure 5 illustrates this feature in greater detail by depicting the evolution of the mass spectrum of asphaltene A1, over 14 mass units. Each peak in the spectra is assigned to a given stoichiometry and the representation then indicates the steady increase of the mass defect with growing mass in each heteroatom class, as a consequence of the increased number of H atoms.

A noticeable similarity can be appreciated in Figure 5 between the spectra of analytes differing in the nominal mass of a CH_2 group (e.g., m/z 450 vs 464, the mass spectra within these two nominal masses virtually overlap when represented in the Kendrick mass scale). All of these features are consistent

with island- and archipielago-type molecular structures, combining polyaromatic cores with hydrocarbon chains.

At this point, we consider the aromatic character of the four crude oil extracts in greater detail. The illustrative spectra and assignments outlined on Figures 4 and 5 show that asphaltenes are typically richer than resins in compounds with small mass defects and, correspondingly, higher DBEs. This already suggests higher abundances of polyaromatic moieties in their constituents. Figure 6 depicts contour plots of the DBEs versus the number of carbon atoms per molecule (n_C), with color codes reflecting relative abundances. Such contour plots are commonly employed in modern petroleomics, because they provide compact overviews of large ensembles of chemical compounds, leading to convenient comparisons between samples.[2−5,66,67,71,72]

Figure 6 corroborates that DBE diagrams conform efficient signatures to discern asphaltenes from resins, as described in the following. The compounds detected in positive-ion mode display differentiated DBE trends in the asphaltene and resin samples. For the two resins, the DBE values observed are comparably low (<20), with an average value of ∼10. Moreover, this average value is weakly dependent on the number of carbons, which indicates that the growth in molecular size is associated with the incorporation of saturated aliphatic units to the molecular structure. In contrast, the DBE
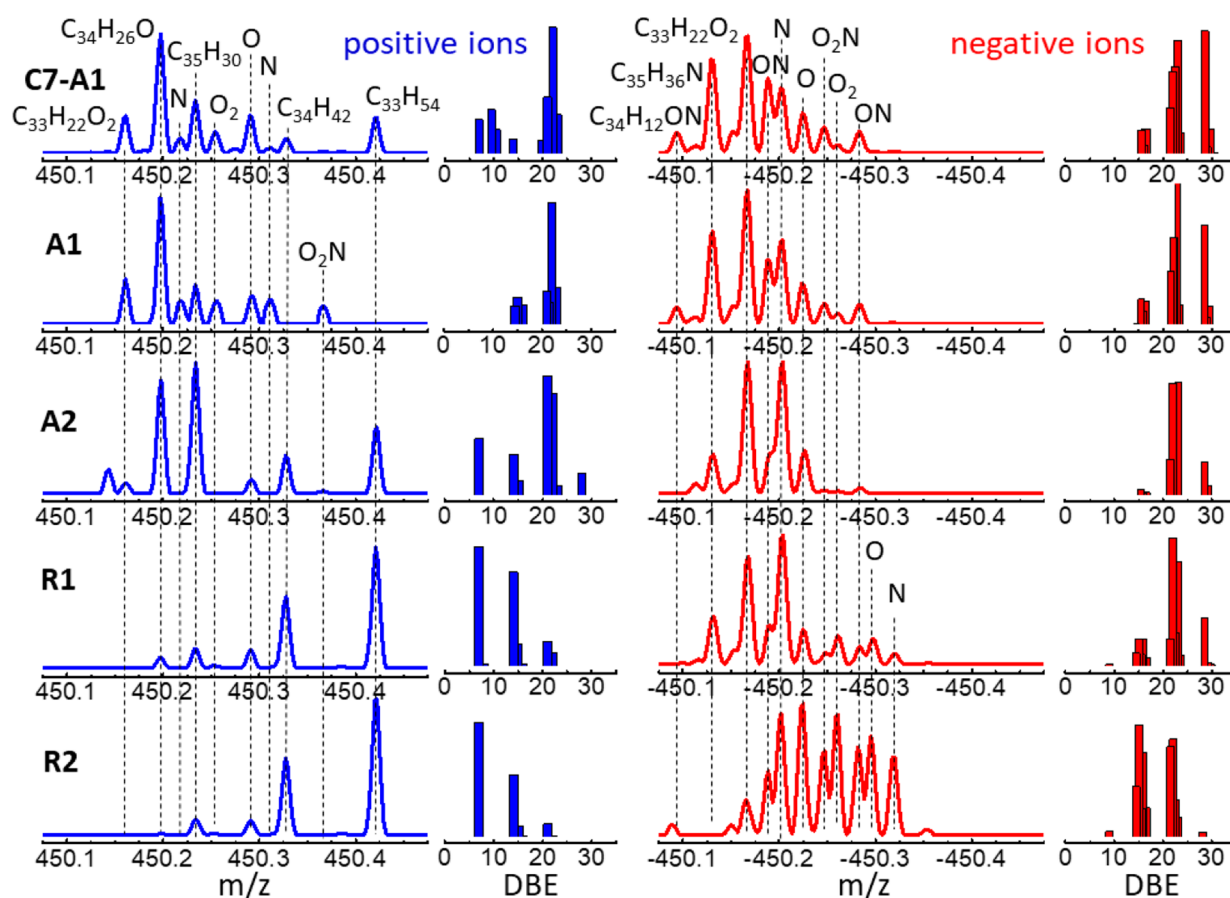
Figure 4. Illustrative assignment of chemical constituents in the APCI-orbitrap mass spectra of the asphaltene (C7-A1, A1, A2) and resin (R1, R2) samples. The heteroatom classes associated with the main peaks in the spectra are indicated; full stoichiometries are indicated for some of the peaks for reference. The bar diagrams represent the relative abundance versus the DBEs associated with the molecular species detected in each spectral window.

of the positive ions of the asphaltenes extends to 30 with a steady growth of the average DBE with the number of carbons (e.g., at $n_C = 20$ and 35, the average DBE values are 12 and 20 for asphaltene A1, and 10 and 24 for asphaltene A2, respectively). Hence, for the asphaltenes, the increase of carbon atoms in the molecules is largely associated with the growth of their polyaromatic cores. Aromaticity is consistently enhanced in the negative ions for the four samples, especially as the number of carbon atoms increases. This can be traced back to the fact that heteroatoms are primarily incorporated in aromatic moieties. Only the less-polar resin fraction R1 maintains a comparably low aromatic character, although even in this case, a neat positive increment of the DBE with n_C is appreciated. The A2 asphaltene fraction displays the most marked aromatic character, reaching DBE values close to 50 in the high n_C end of the distribution. This finding is consistent with the lower H/C ratio derived from elemental analysis (see Table 2).

To provide a compact characterization of the overall chemical composition of the crude oil fractions, the species identified in the APCI-orbitrap mass spectra are sorted out in Figure 7, according to their weighted average heteroatom content, into O_x, N_y, N_yO_x, and CH (no heteroatom) classes. This type of data reduction is commonly employed in petroleomics.[2−5] In consonance with the illustrative mass spectral ranges discussed above, the chemical species detected in positive-ion mode display significantly lower heteroatom

contents than their negative-ion counterparts. For the two resin fractions, roughly 90% of the compounds detected in positive-ion mode belong to the CH class, which contains no heteroatoms. Interestingly, the CH class is also dominant in the positive ions of the A2 asphaltene fraction (65%), although this asphaltene displays a significantly enhanced abundance of O_x species (23%), compared to the resin fractions (<10%). The positive ions of the A1 asphaltene are spread over different heteroatom classes; the O and O_2 heteroatom classes are most abundant (ca. 47%), while the presence of CH compounds is appreciable as well (28%). The A1 products detected in negative-ion mode are richer in heteroatom content and further expose the chemical diversity of the components of the crude oil fractions. In this case, the dominant O and O_2 species account for a joint abundance of 58% and most of the remaining 42% is distributed among the N and NO_x classes. In the A2 asphaltene in the negative-ion mode, the O and O_2 classes are clearly dominant, with 87% of joint relative abundance. Hence, the A2 asphaltene is primarily conformed by polyaromatic hydrocarbons and their O-containing derivatives. Note that such marked abundance of O_x classes is consistent with the large O content, of up to 14 wt %, inferred from the elemental analysis of the A2 asphaltene (see Table 2). The R1 and R2 resin fractions both show broad distributions of heteroatomic classes, although with quantitative differences related to their different abundances in O_x compounds (70% in resin R1 vs 56% in resin R2) and in N-
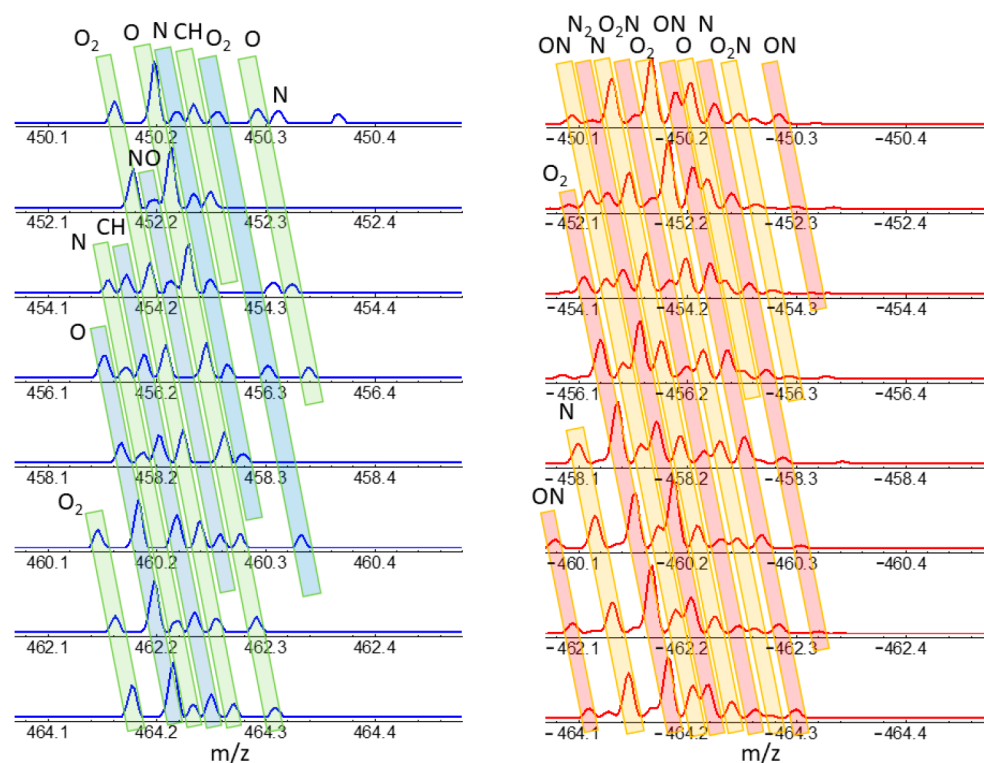
Figure 5. Identification of homologue heteroatom sequences illustrated for the APCI-orbitrap spectra recorded for the A1 asphaltene, in positive and negative ion modes (blue and red spectral traces, respectively). Spectra are shown in intervals of 2 mass units (loss or gain of two H atoms, associated with single-bond/double-bond substitutions in the molecular structure). The bands with alternating colors are meant to highlight the evolution of the peaks associated any given heteroatom class. Note the coincidence in the overall shape of the mass spectra separated by 14 nominal mass units (hence showing compounds with structures differing in one CH_2 group; consequently, the spectra overlap if represented in terms of the Kendrick mass scale (not shown)).
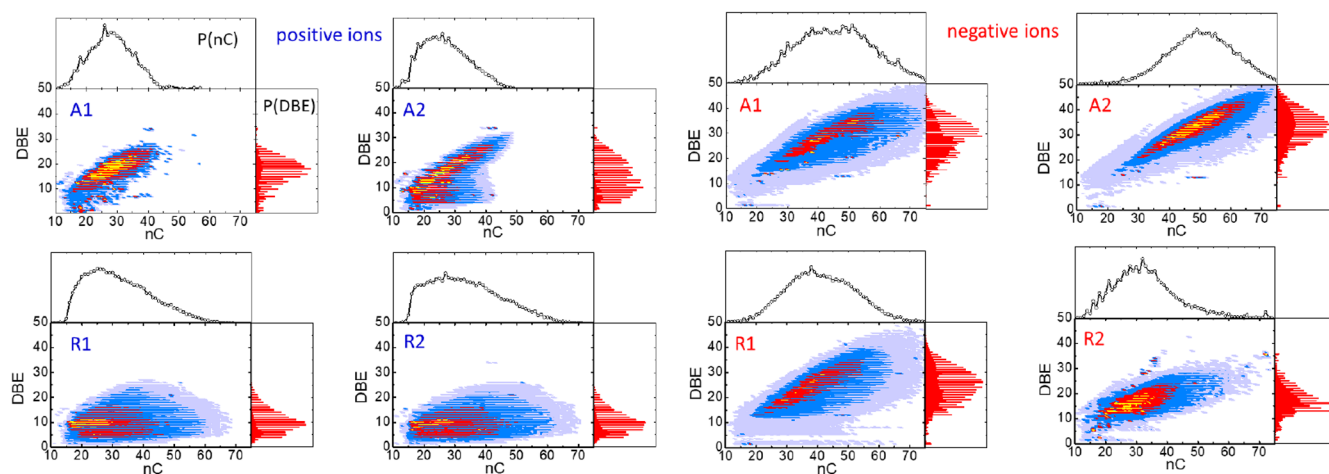

Figure 6. :Contour plots mapping the DBEs versus number of carbon atoms for the compounds assigned in the APCI-orbitrap spectra of the asphaltenes (A1, A2) and resins (R1, R2). The top and side layers of each frame depict the integrated carbon number and DBE probability distributions, respectively.

containing N/NO_x compounds (28% in resin R1 vs 42% in resin R2).

We close the discussion of the APCI-orbitrap spectra with considerations regarding the results for the *n*-heptane-extracted asphaltenes from deposit DP1 (C_7-A1 asphaltenes), in comparison to the *n*-hexane asphaltenes A1 just discussed. Figure 4 illustrates the small differences observed in the mass spectra of the two asphaltene fractions. The negative-ion mode spectra are close matching over the whole spectral range,

showing coincidence in the detected species with small quantitative variations in their relative intensities. The positive-ion spectra are as well largely coincident, although, in this case, some sizable differences in the ensemble of compounds detected in each fraction are observed, in particular for CH class compounds. The class distributions depicted in Figure 7 reveal that the abundance of heteroatomic species in both positive- and negative-ion modes is greater for the A1 asphaltene in comparison to the C_7-A1 asphaltene, as
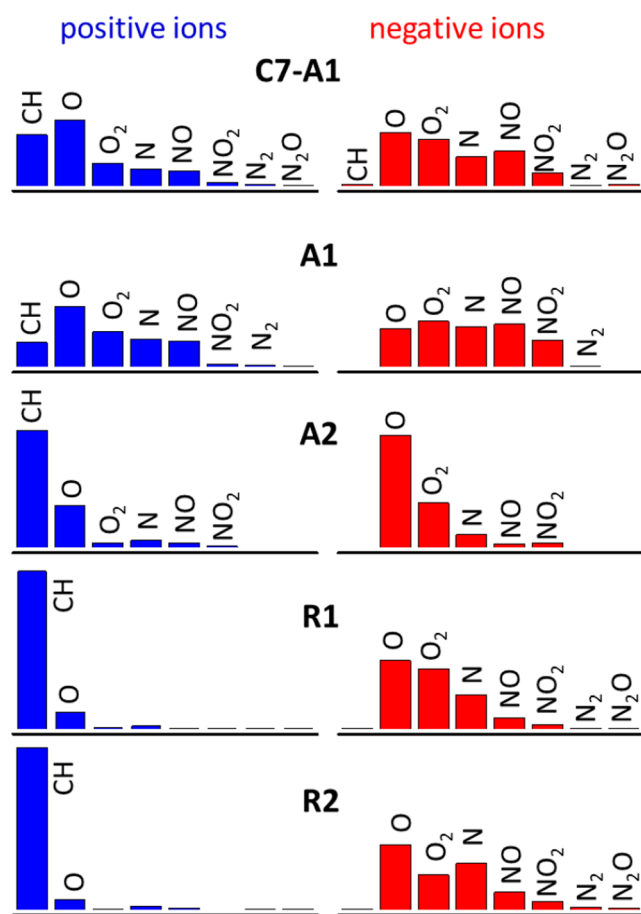
Figure 7. Relative abundances of the heteroatom classes, O_x, N_y, O_xN_y, and CH (no heteroatoms), as derived from the APCI-orbitrap mass spectra of the asphaltene (C7-A1, A1, A2) and resin (R1,R2) extracts.

would be expected for a *n*-hexane vs *n*-heptane extraction, although the difference is not large. These findings should be revisited in future investigations with a broader range of ionizing techniques (e.g., ESI and APPI).

3.4. LDI-TOF Mass Spectra. LDI-TOF mass spectrometry has been extensively used in petroleum analysis over the past two decades. As a main advantage, it achieves a soft ionization over a broad range of molecular weights for analytes embedded in light-absorbing matrices. LDI yields typically strong signals for crude oil extracts, because of their facile absorption of UV-vis or infrared (IR) light.[50,74−83] A major challenge in LDI mass spectrometry analysis of asphaltenes is related to the difficulty of discerning between monomeric molecular species and their noncovalent aggregates. In LDI, the laser is typically applied to solid asphaltene or resin samples (in the form of powder, or of precipitate produced after evaporation of the solvent). Whereas the solid material sublimates upon laser heating, the density of the desorption plume is sufficiently high for many-body collisions to stabilize supramolecular aggregates as the plume expands and cools down. As a result, LDI mass spectra of crude oil extracts may extend over several thousand daltons. Figure 8 depicts the LDI-TOF mass spectra recorded for the asphaltenes and resins object of the present study. Asphaltenes A1 and A2 display broad LDI mass spectra, peaking slightly above 2000 Da and extending above 4000 Da. Resins R1 and R2 show narrower LDI distributions, although

with long tails reaching 2000 Da. It is well-stablished that asphaltenes are more prone to aggregate than resins, which is consistent with the broader LDI mass distributions. Many works have reviewed comprehensively aggregation effects in LDI mass spectrometry of asphaltenes.[50,75,72−78] This study will rather focus on the degree of coincidence in the molecular species detected with the LDI-TOF and the APCI-orbitrap techniques, in the mass region where both signals overlap.

Figure 8 presents a comparison of the LDI and APCI spectra measured for the four samples. An overall coincidence is found between the ion trends generated by the LDI and APCI techniques for the asphaltene and resin samples at molecular weights up to 600 Da. It can be observed that the LDI spectra display similar recurrent peak sequences as their APCI counterparts, with periodicities of 14 Da (CH_2) and 2 Da (2H). Moreover, the detailed inspection over single nominal masses reveals that the position and relative intensities of the high-resolution orbitrap peaks are, to a large extent, consistent with the envelopes of the broader TOF peaks. Nevertheless, systematic differences are also appreciated between the spectra generated by the APCI and LDI techniques. On the one hand, LDI yields an excess of signal of products with small mass defects (<0.2 Da), hence, those associated with H-deficient polyaromatic core structures. This is, for instance, the case for the peaks tentatively assigned to $C_{35}H_{14}O$, $C_{40}H_{20}$, and $C_{44}H_{22}$ (with DBE = 29, 31, and 34, respectively) in the spectra of the two asphaltenes depicted in Figure 8. For the A2 fraction, the differences are more appreciable than for the A1 fraction, and they extend to products of lower aromaticity (e.g., $C_{41}H_{48}$, with DBE = 18). On the other hand, the mass spectra of the two resins suggest that LDI largely underestimates the peak intensities at high mass defects (>0.4 Da), which can be traced back to a low sensitivity toward compounds of low aromaticity and marked aliphatic character. In the illustrative examples of Figure 8, this is the case for the peaks assigned to $C_{33}H_{54}$, $C_{36}H_{68}$, or $C_{39}H_{72}$ (with DBE = 7, 3 and 4, respectively) in the mass spectra of the R1 and R2 resin fractions.

Summarizing, there is substantial overlap between the ensembles of molecular ions produced by the LDI and APCI techniques, up to molecular weights of ∼600 Da. The large optical absorbance of the resin and asphaltene matrices assists the ionization of a broad range of molecular components for which direct laser ionization is less efficient. Nevertheless, a trend for an enhanced ionization of polyaromatic (large DBE), and for a reduced sensitivity toward more aliphatic (small DBE) architectures, is observed in LDI vs APCI.

4. GENERAL REMARKS AND CONCLUSIONS

Asphaltene and resin fractions from Algerian Hassi−Messaoud crude oil have been characterized at a molecular level by means of high-resolution mass spectrometry. The asphaltene fractions are considered nonstable, with respect to precipitation, because they were extracted from two different deposits collected at the production and storage stages of the crude oil. The latter fraction (A2) is comparably less stable than the former fraction (A1), according to the lower aggregation onset observed in this study. The resin fractions were obtained directly from the crude oil and are considered as stabilizers regarding asphaltenes aggregation.

APCI-orbitrap mass spectrometry has been applied to characterize the molecular composition of the asphaltene and resin samples. The identification of positive and negative ionic
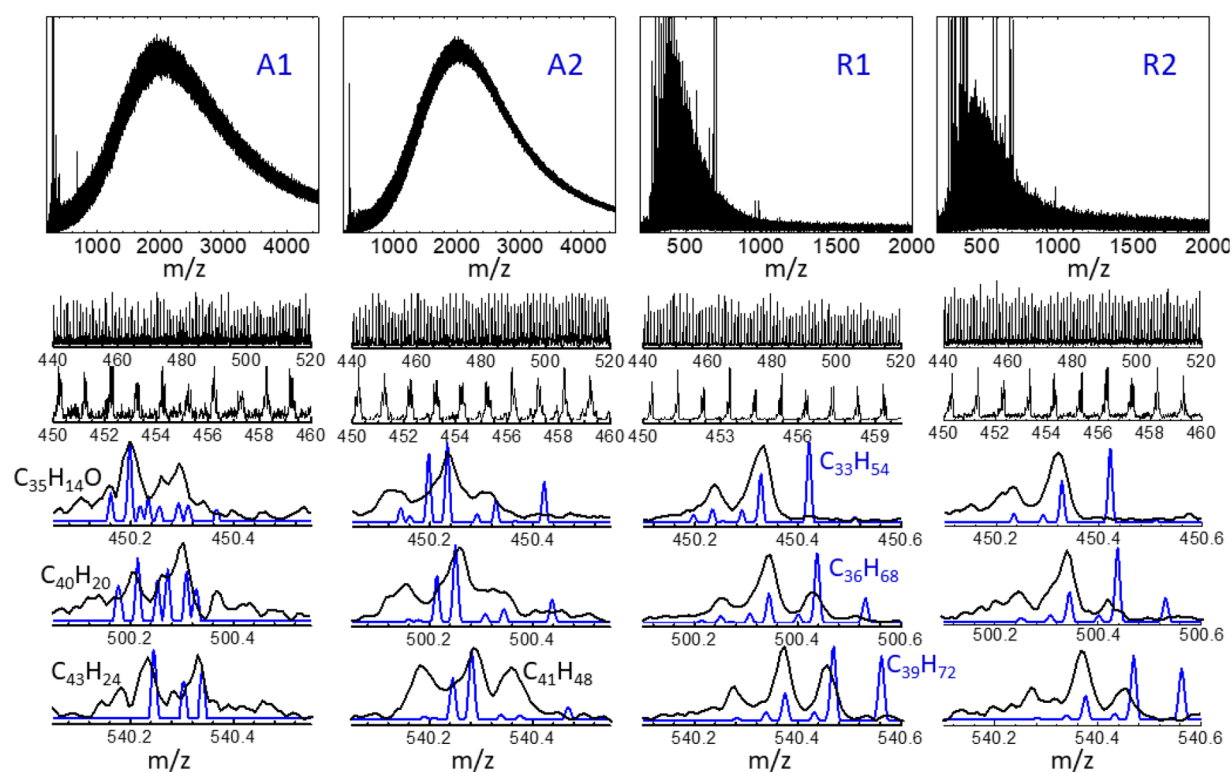
Figure 8. LDI-TOF spectra (black traces) of the asphaltene (A1, A2) and resin (R1, R2) extracts of crude oil. The spectra are shown at different levels of amplification of the mass range, in a similar way as in Figure 3. The three lower panels for each sample show a comparison with the corresponding APCI-orbitrap spectra (blue traces). The assignment indicated for some of the peaks serves to highlight the different ionization efficiencies of the LDI and APCI techniques (see text).

species has served to expose a diversity of species with varying heteroatom content and overall basic and acidic character. In general terms, the present study extends earlier studies of the composition and structural properties of Algerian asphaltenes, using lower resolution mass spectrometry and spectroscopic methods (FT-IR and NMR),[57] and corroborates the suggested changes in composition and aggregation propensity during the early stages of crude oil transportation and processing.

The main results of the present investigation may be summarized as follows:

● The deposit DP1 formed at the production well yields 88 wt % of n-hexane asphaltenes (A1) and is plausibly related to flocculation induced by the hydrocarbon content of the lift gas employed for enhanced oil recovery. According to the present analysis, the A1 asphaltenes display a broad heteroatom class composition, with a roughly even contribution from O- and N-containing compounds and an appreciable polyaromatic character (average DBE of 16 and 28, for the positive and negative ions, respectively).

● The asphaltene fraction from deposit DP2, formed at the downstream storage tank, yields 85 wt % of n-hexane asphaltenes (A2). A characteristic feature of the A2 asphaltenes is a large oxygen content, of as much as 14% according to the evidence provided by the elemental analysis. Consistently, the mass spectrometry analysis indicates a dominant abundance of the O-containing heteroatom classes (the O and O_2 classes account for 80% of the negative ions detected). The processes leading to this apparent overoxygenation of the DP2 material are currently uncertain and will be a topic of future research. The A2 fraction also features a greater abundance of native hydrocarbons (CH class) and a significant overall polyaromatic

character (average DBE of 15 and 33 for the positive and negative ions, respectively). The large O content and aromaticity correlate with a marked propensity for aggregation in the A2 asphaltenes, as derived from its comparably small aggregation onset, of 55 vol % of hexane/toluene solution versus 72 vol % for A1.

● The resin fractions of the Hassi–Messaoud crude oil are found to be abundant in aliphatic hydrocarbons and heteroatomic compounds of moderate aromaticity. The more polar resin fraction, R2, is enriched in O_x classes (56%) and markedly in N-containing species (42%), with respect to the less-polar resin fraction R1 (28%). These results suggest a stronger interaction of the R2 resin fraction with asphaltenes, potentially leading to enhanced stabilization effects, consistent with previous observations.[34]

The application of LDI-TOF mass spectrometry to the samples yields high mass signals that are plausibly related, to an uncertain extent, to supramolecular aggregates. Nevertheless, at low masses (<600 Da), the bands observed in the LDI-TOF mass spectra are, to a large extent, consistent with the ensembles of molecular ions produced with APCI. Nevertheless, the comparison of the spectra produced with two techniques suggests that LDI, in comparison to APCI, enhances the ionization of polyaromatic, plausibly "island-like", compounds of asphaltenes with large DBE, whereas it yields a reduced sensitivity toward more aliphatic species, with saturated side chains and a comparably smaller DBE.

This study constitutes an approximation to the detailed composition of Algerian Hassi–Messaoud crude oil. Further investigation is required to progress in the elucidation of the molecular properties that affect its stability and the

precipitation of its asphaltene fraction. In particular, detailed insights into the role of the dominant molecular structures in the aggregation of asphaltenes, e.g., island versus archipielago architectures, would require extensive subfractionation prior to mass spectrometry analysis and plausibly a combination of different ionization techniques.[3] Future work in our group will follow that strategy and will furthermore investigate the selective precipitation and flocculation of asphaltene subfractions in the presence of resin fractions of different polarity.

■ AUTHOR INFORMATION

Corresponding Author

　　Mortada Daaou − *LCPM, Département de Chimie, Faculté des Sciences Université d'Oran 1 (Ahmed Benbella), Oran 31000, Algeria; LSPBE, Département de Génie Chimique, Faculté de Chimie, Université des Sciences et de la Technologie d'Oran- Mohamed Boudiaf, Oran 31000, Algeria;* ⬤ orcid.org/0000-0002-9343-4742; Email: daaou_mortada@yahoo.fr

Authors

　　Fatima Saad − *LCPM, Département de Chimie, Faculté des Sciences Université d'Oran 1 (Ahmed Benbella), Oran 31000, Algeria*

　　Boumedienne Bounaceur − *LCPM, Département de Chimie, Faculté des Sciences Université d'Oran 1 (Ahmed Benbella), Oran 31000, Algeria*

　　Juan Ramón Avilés-Moreno − *Department of Applied Physical Chemistry, Universidad Autónoma de Madrid, 28049 Madrid, Spain*

　　Bruno Martínez-Haya − *Department of Physical, Chemical and Natural Systems, Universidad Pablo de Olavide, 41013 Seville, Spain;* ⬤ orcid.org/0000-0003-2682-3286

Complete contact information is available at:
https://pubs.acs.org/10.1021/acs.energyfuels.1c00333

Notes

The authors declare no competing financial interest.

■ ACKNOWLEDGMENTS

■ REFERENCES

(1) Marshall, A. G.; Rodgers, R. P. Petroleomics: The Next Grand Challenge for Chemical Analysis. *Acc. Chem. Res.* **2004**, 37 (1), 53−59.

(2) Chacón-Patiño, M. L.; Rowland, S. M.; Rodgers, R. P. Advances in Asphaltene Petroleomics. Part 1: Asphaltenes Are Composed of Abundant Island and Archipelago Structural Motifs. *Energy Fuels* **2017**, 31 (12), 13509−13518.

(3) Chacón-Patiño, M. L.; Rowland, S. M.; Rodgers, R. P. Advances in Asphaltene Petroleomics. Part 2: Selective Separation Method That Reveals Fractions Enriched in Island and Archipelago Structural Motifs by Mass Spectrometry. *Energy Fuels* **2018**, 32 (1), 314−328.

(4) Chacón-Patiño, M. L.; Rowland, S. M.; Rodgers, R. P. Advances in Asphaltene Petroleomics. Part 3. Dominance of Island or Archipelago Structural Motif Is Sample Dependent. *Energy Fuels* **2018**, 32 (9), 9106−9120.

(5) Chacón-Patiño, M. L.; Smith, D. F.; Hendrickson, C. L.; Marshall, A. G.; Rodgers, R. P. Advances in Asphaltene Petroleomics. Part 4. Compositional Trends of Solubility Subfractions Reveal That Polyfunctional Oxygen-Containing Compounds Drive Asphaltene Chemistry. *Energy Fuels* **2020**, 34 (3), 3013−3030.

(6) Schuler, B.; Fatayer, S.; Meyer, G.; Rogel, E.; Moir, M.; Zhang, Y.; Harper, M. R.; Pomerantz, A. E.; Bake, K. D.; Witt, M.; Peña, D.; Kushnerick, J. D.; Mullins, O. C.; Ovalles, C.; van den Berg, F. G. A.; Gross, L. Heavy Oil Based Mixtures of Different Origins and Treatments Studied by Atomic Force Microscopy. *Energy Fuels* **2017**, 31 (7), 6856−6861.

(7) Zheng, F.; Shi, Q.; Vallverdu, G. S.; Giusti, P.; Bouyssiere, B. Fractionation and Characterization of Petroleum Asphaltene: Focus on Metalopetroleomics. *Processes* **2020**, 8, 1504.

(8) Vargas, F. M.; Creek, J. L.; Chapman, W. G. On the Development of an Asphaltene Deposition Simulator. *Energy Fuels* **2010**, 24, 2294−2299.

(9) Haskett, C. E.; Tartera, M. A Practical Solution to the Problem of Asphaltene Deposits. *JPT, J. Pet. Technol.* **1965**, 17 (04), 387−391.

(10) Hamadou, R.; Khodja, M.; Kartout, M.; Jada, A. Permeability Reduction by Asphaltenes and Resins Deposition in Porous Media. *Fuel* **2008**, 87 (10−11), 2178−2185.

(11) Hammami, A.; Ratulowski, J. Precipitation and Deposition of Asphaltenes in Production Systems: A Flow Assurance Overview. *In Asphaltenes, Heavy Oils, and Petroleomics* **2007**, 617−660.

(12) Porte, G.; Zhou, H.; Lazzeri, V. Reversible Description of Asphaltene Colloidal Association and Precipitation. *Langmuir* **2003**, 19 (1), 40−47.

(13) Carbognani, L.; Orea, M.; Fonseca, M. Complex Nature of Separated Solid Phases from Crude Oils. *Energy Fuels* **1999**, 13 (2), 351−358.

(14) Rogel, E.; León, O.; Torres, G.; Espidel, J. Aggregation of Asphaltenes in Organic Solvents Using Surface Tension Measurements. *Fuel* **2000**, 79 (11), 1389−1394.

(15) Amjad-Iranagh, S.; Rahmati, M.; Haghi, M.; Hoseinzadeh, M.; Modarress, H. Asphaltene Solubility in Common Solvents: A Molecular Dynamics Simulation Study. *Can. J. Chem. Eng.* **2015**, 93 (12), 2222−2232.

(16) Yen, T. F.; Chilingarian, G. V. Asphaltenes and Asphalts, 2. *Dev. Pet. Sci.* **2000**, 40 (PART B), 1−5.

(17) Mullins, O. C. The Asphaltenes. *Annu. Rev. Anal. Chem.* **2011**, 4, 393−418.

(18) Mullins, O. C. The Modified Yen Model. *Energy Fuels* **2010**, 24, 2179−2207.

(19) Daaou, M.; Modarressi, A.; Bendedouch, D.; Bouhadda, Y.; Krier, G.; Rogalski, M. Characterization of the Nonstable Fraction of Hassi-Messaoud Asphaltenes. *Energy Fuels* **2008**, 22 (5), 3134−3142.

(20) Larbi, A.; Daaou, M.; Faraoun, A. Investigation of Structural Parameters and Self-Aggregation of Algerian Asphaltenes in Organic Solvents. *Pet. Sci.* **2015**, 12 (3), 509−517.

(21) Castellano, O.; Gimon, R.; Canelon, C.; Aray, Y.; Soscun, H. Molecular Interactions between Orinoco Belt Resins. *Energy Fuels* **2012**, 26, 2711−2720.

(22) Dufour, J.; Calles, J. A.; Marugán, J.; Giménez-Aguirre, R.; Peña, J. L.; Merino-García, D. Influence of Hydrocarbon Distribution in Crude Oil and Residues on Asphaltene Stability. *Energy Fuels* **2010**, 24, 2281−2286.

(23) Goual, L.; Firoozabadi, A. Effect of Resins and DBSA on Asphaltene Precipitation from Petroleum Fluids. *AIChE J.* **2004**, 50 (2), 470−479.

(24) Sedghi, M.; Goual, L. Role of Resins on Asphaltene Stability. *Energy Fuels* **2010**, 24, 2275−2280.

(25) León, O.; Contreras, E.; Rogel, E.; Dambakli, G.; Acevedo, S.; Carbognani, L.; Espidel, J. Adsorption of Native Resins on Asphaltene Particles: A Correlation between Adsorption and Activity. *Langmuir* **2002**, 18 (13), 5106−5112.

(26) Rogel, E. Molecular Thermodynamic Approach to the Formation of Mixed Asphaltene-Resin Aggregates. *Energy Fuels* **2008**, 22 (6), 3922−3929.

(27) Andersen, S. I.; Speight, J. G. Petroleum Resins: Separation, Character, and Role in Petroleum. *Pet. Sci. Technol.* **2001**, *19* (1−2), 1−34.

(28) Carnahan, N. F.; Salager, J. L.; Antón, R.; Dávila, A. Properties of Resins Extracted from Boscan Crude Oil and Their Effect on the Stability of Asphaltenes in Boscan and Hamaca Crude Oils. *Energy Fuels* **1999**, *13* (2), 309−314.

(29) León, O.; Rogel, E.; Espidel, J.; Torres, G. Asphaltenes: Structural Characterization, Self-Association, and Stability Behavior. *Energy Fuels* **2000**, *14* (1), 6−10.

(30) Taylor, S. E. The Electrodeposition of Asphaltenes and Implications for Asphaltene Structure and Stability in Crude and Residual Oils. *Fuel* **1998**, *77* (8), 821−828.

(31) Wang, J.; Buckley, J. S. Asphaltene Stability in Crude Oil and Aromatic Solvents - The Influence of Oil Composition. *Energy Fuels* **2003**, *17* (6), 1445−1451.

(32) Spiecker, P. M.; Gawrys, K. L.; Trail, C. B.; Kilpatrick, P. K. Effects of Petroleum Resins on Asphaltene Aggregation and Water-in-Oil Emulsion Formation. *Colloids Surf., A* **2003**, *220* (1−3), 9−27.

(33) Ortega-Rodríguez, A.; Cruz, S. A.; Gil-Villegas, A.; Guevara-Rodríguez, F.; Lira-Galeana, C. Molecular View of the Asphaltene Aggregation Behavior in Asphaltene-Resin Mixtures. *Energy Fuels* **2003**, *17* (4), 1100−1108.

(34) Faraoun, A.; Daaou, M.; Bounaceur, B. Use of Surfactants to Mitigate Precipitation of Nonstable Asphaltenes. *Energy Sources, Part A* **2016**, *38* (19), 2830−2836.

(35) Derakhshani-Molayousefi, M.; McCullagh, M. Deterring Effect of Resins on the Aggregation of Asphaltenes in N-Heptane. *Energy Fuels* **2020**, *34* (12), 16081−16088.

(36) Koots, J. A.; Speight, J. G. Relation of Petroleum Resins to Asphaltenes. *Fuel* **1975**, *54* (3), 179−184.

(37) Murgich, J.; Rodríguez M, J.; Aray, Y. Molecular Recognition and Molecular Mechanics of Micelles of Some Model Asphaltenes and Resins. *Energy Fuels* **1996**, *10* (1), 68−76.

(38) Andersen, S. I.; Speight, J. G. Petroleum Resins: Separation, Character, and Role in Petroleum. *Pet. Sci. Technol.* **2001**, *19* (1−2), 1−34.

(39) Pomerantz, A. E.; Mullins, O. C.; Paul, G.; Ruzicka, J.; Sanders, M. Orbitrap Mass Spectrometry: A Proposal for Routine Analysis of Nonvolatile Components of Petroleum. *Energy Fuels* **2011**, *25*, 3077−3082.

(40) Smith, E. A.; Lee, Y. J. Petroleomic Analysis of Bio-Oils from the Fast Pyrolysis of Biomass: Laser Desorption Ionization-Linear Ion Trap-Orbitrap Mass Spectrometry Approach. *Energy Fuels* **2010**, *24*, 5190−5198.

(41) Santos, J. M.; Vetere, A.; Wisniewski, A.; Eberlin, M. N.; Schrader, W. Modified SARA Method to Unravel the Complexity of Resin Fraction(s) in Crude Oil. *Energy Fuels* **2020**, *34* (12), 16006−16013.

(42) Xian, F.; Hendrickson, C. L.; Marshall, A. G. High Resolution Mass Spectrometry. *Anal. Chem.* **2012**, *84* (2), 708−719.

(43) Zhurov, K. O.; Kozhinov, A. N.; Tsybin, Y. O. Evaluation of High-Field Orbitrap Fourier Transform Mass Spectrometer for Petroleomics. *Energy Fuels* **2013**, *27* (6), 2974−2983.

(44) Martins, L. L.; Angolini, C. F. F.; da Cruz, G. F.; Marsaioli, A. J. Characterization of Acidic Compounds in Brazilian Tar Sand Bitumens by LTQ Orbitrap XL: Assessing Biodegradation Using Petroleomics. *J. Braz. Chem. Soc.* **2016**, *28* (5), 848−857.

(45) Nyadong, L.; Lai, J.; Thompsen, C.; Lafrancois, C. J.; Cai, X.; Song, C.; Wang, J.; Wang, W. High-Field Orbitrap Mass Spectrometry and Tandem Mass Spectrometry for Molecular Characterization of Asphaltenes. *Energy Fuels* **2018**, *32* (1), 294−305.

(46) Schmidt, E. M.; Pudenzi, M. A.; Santos, J. M.; Angolini, C. F. F.; Pereira, R. C. L.; Rocha, Y. S.; Denisov, E.; Damoc, E.; Makarov, A.; Eberlin, M. N. Petroleomics via Orbitrap Mass Spectrometry with Resolving Power above 1.000.000 at m/z 200. *RSC Adv.* **2018**, *8* (11), 6183−6191.

(47) Palacio Lozano, D. C.; Thomas, M. J.; Jones, H. E.; Barrow, M. P. Petroleomics: Tools, Challenges, and Developments. *Annu. Rev. Anal. Chem.* **2020**, *13*, 405−430.

(48) Witt, M.; Godejohann, M.; Oltmanns, S.; Moir, M.; Rogel, E. Characterization of Asphaltenes Precipitated at Different Solvent Power Conditions Using Atmospheric Pressure Photoionization (APPI) and Laser Desorption Ionization (LDI) Coupled to Fourier Transform Ion Cyclotron Resonance Mass Spectrometry (FT-ICR MS). *Energy Fuels* **2018**, *32* (3), 2653−2660.

(49) Chacón-Patiño, M. L.; Vesga-Martínez, S. J.; Blanco-Tirado, C.; Orrego-Ruiz, J. A.; Gómez-Escudero, A.; Combariza, M. Y. Exploring Occluded Compounds and Their Interactions with Asphaltene Networks Using High-Resolution Mass Spectrometry. *Energy Fuels* **2016**, *30* (6), 4550−4561.

(50) Martínez-Haya, B.; Hortal, A. R.; Hurtado, P.; Lobato, M. D.; Pedrosa, J. M. Laser Desorption/Ionization Determination of Molecular Weight Distributions of Polyaromatic Carbonaceous Compounds and Their Aggregates. *J. Mass Spectrom.* **2007**, *42* (6), 701−713.

(51) Sjovall, P.; Bake, K. D.; Pomerantz, A. E.; Lu, X.; Mitra-Kirtley, S.; Mullins, O. C. Analysis of kerogens and model compounds by time-of-flight secondary ion mass spectrometry (TOF-SIMS). *Fuel* **2021**, *286*, 119373.

(52) Daaou, M.; Bendedouch, D.; Modarressi, A.; Rogalski, M. Properties of the Polar Fraction of Hassi-Messaoud Asphaltenes. *Energy Fuels* **2012**, *26* (9), 5672−5678.

(53) Souas, F.; Safri, A.; Benmounah, A.; EddineDjemiat, D. Rheological Behavior of Algerian Crude Oil: Effect of Temperature and Refined Product. *Pet. Sci. Technol.* **2018**, *36* (21), 1757−1763.

(54) Djemiat, D. E.; Safri, A.; Benmounah, A.; Safi, B. Rheological Behavior of an Algerian Crude Oil Containing Sodium Dodecyl Benzene Sulfonate (SDBS) as a Surfactant: Flow Test and Study in Dynamic Mode. *J. Pet. Sci. Eng.* **2015**, *133*, 184−191.

(55) Behnous, D.; Palma, A.; Zeraibi, N.; Coutinho, J. A. P. Modeling Asphaltene Precipitation in Algerian Oilfields with the CPA EoS. *J. Pet. Sci. Eng.* **2020**, *190*, 107−115.

(56) Daaou, M.; Bendedouch, D. Water PH and Surfactant Addition Effects on the Stability of an Algerian Crude Oil Emulsion. *J. Saudi Chem. Soc.* **2012**, *16* (3), 333−337.

(57) Bouhadda, Y.; Bormann, D.; Sheu, E.; Bendedouch, D.; Krallafa, A.; Daaou, M. Characterization of Algerian Hassi-Messaoud Asphaltene Structure Using Raman Spectrometry and X-Ray Diffraction. *Fuel* **2007**, *86* (12−13), 1855−1864.

(58) Daaou, M.; Bendedouch, D.; Bouhadda, Y.; Vernex-Loset, L.; Modaressi, A.; Rogalski, M. Explaining the Flocculation of Hassi-Messaoud Asphaltenes in Terms of Structural Characteristics of Monomers and Aggregates. *Energy Fuels* **2009**, *23* (11), 5556−5563.

(59) Daaou, M.; Larbi, A.; Martínez-Haya, B.; Rogalski, M. A Comparative Study of the Chemical Structure of Asphaltenes from Algerian Petroleum Collected at Different Stages of Extraction and Processing. *J. Pet. Sci. Eng.* **2016**, *138*, 50−56.

(60) ASTM Standard D2007-03, Standard Test Method for Characteristic Groups in Rubber Extender and Processing Oils and Other Petroleum-Derived Oils by the Clay-Gel Absorption Chromatographic Method. In *2008 ASTM Annual Book of Standards*; American Society for Testing and Materials: West Conshohocken, PA, 2008; available via the Internet at: www.astm.org.

(61) Zuth, C.; Vogel, A. L.; Ockenfeld, S.; Huesmann, R.; Hoffmann, T. Ultrahigh-Resolution Mass Spectrometry in Real Time: Atmospheric Pressure Chemical Ionization Orbitrap Mass Spectrometry of Atmospheric Organic Aerosol. *Anal. Chem.* **2018**, *90* (15), 8816−8823.

(62) Cunico, R. L.; Sheu, E. Y.; Mullins, O. C. Molecular Weight Measurement of UG8 Asphaltene Using APCI Mass Spectroscopy. *Pet. Sci. Technol.* **2004**, *22*, 787−798.

(63) Gao, J.; Borton, D. J.; Owen, B. C.; Jin, Z.; Hurt, M.; Amundson, L. M.; Madden, J. T.; Qian, K.; Kenttämaa, H. I. Laser-Induced Acoustic Desorption/ Atmospheric Pressure Chemical

Ionization Mass Spectrometry. *J. Am. Soc. Mass Spectrom.* **2011**, *22* (3), 531−538.

(64) Owen, B. C.; Gao, J.; Borton, D. J.; Amundson, L. M.; Archibold, E. F.; Tan, X.; Azyat, K.; Tykwinski, R.; Gray, M.; Kenttämaa, H. I. Carbon Disulfide Reagent Allows the Characterization of Nonpolar Analytes by Atmospheric Pressure Chemical Ionization Mass Spectrometry. *Rapid Commun. Mass Spectrom.* **2011**, *25* (14), 1924−1928.

(65) Hurt, M. R.; Borton, D. J.; Choi, H. J.; Kenttämaa, H. I. Comparison of the Structures of Molecules in Coal and Petroleum Asphaltenes by Using Mass Spectrometry. *Energy Fuels* **2013**, *27* (7), 3653−3658.

(66) Klein, G. C.; Kim, S.; Rodgers, R. P.; Marshall, A. G.; Yen, A.; Asomaning, S. Mass Spectral Analysis of Asphaltenes. I. Compositional Differences between Pressure-Drop and Solvent-Drop Asphaltenes Determined by Electrospray Ionization Fourier Transform Ion Cyclotron Resonance Mass Spectrometry. *Energy Fuels* **2006**, *20* (5), 1965−1972.

(67) McLafferty, F. W.; Turecek, F. W. Appendix—Interpretation of Mass Spectra. In *Interpretation of Mass Spectra*, 4th Edition; University Science Books: Mill Valley, CA, 1993.

(68) Kendrick, E. A Mass Scale Based on CH2 = 14.0000 for High Resolution Mass Spectrometry of Organic Compounds. *Anal. Chem.* **1963**, *35* (13), 2146−2154.

(69) Sleno, L. The Use of Mass Defect in Modern Mass Spectrometry. *J. Mass Spectrom.* **2012**, *47* (2), 226−236.

(70) Bouhadda, Y.; Bendedouch, D.; Sheu, E.; Krallafa, A. Some Preliminary Results on a Physico-Chemical Characterization of a HassiMessaoud Petroleum Asphaltene. *Energy Fuels* **2000**, *14* (4), 845−853.

(71) Hughey, C. A.; Hendrickson, C. L.; Rodgers, R. P.; Marshall, A. G.; Qian, K. Kendrick Mass Defect Spectrum: A Compact Visual Analysis for Ultrahigh-Resolution Broadband Mass Spectra. *Anal. Chem.* **2001**, *73* (19), 4676−4681.

(72) Smith, D. F.; Rahimi, P.; Teclemariam, A.; Rodgers, R. P.; Marshall, A. G. Characterization of Athabasca Bitumen Heavy Vacuum Gas Oil Distillation Cuts by Negative/Positive Electrospray Ionization and Automated Liquid Injection Field Desorption Ionization Fourier Transform Ion Cyclotron Resonance Mass Spectrometry. *Energy Fuels* **2008**, *22* (5), 3118−3125.

(73) Rüger, C. P.; Neumann, A.; Sklorz, M.; Schwemer, T.; Zimmermann, R. Thermal Analysis Coupled to Ultrahigh Resolution Mass Spectrometry with Collision Induced Dissociation for Complex Petroleum Samples: Heavy Oil Composition and Asphaltene Precipitation Effects. *Energy Fuels* **2017**, *31* (12), 13144−13158.

(74) Acevedo, S.; Gutierrez, L. B.; Negrin, G.; Pereira, J. C.; Mendez, B.; Delolme, F.; Dessalces, G.; Broseta, D. Molecular Weight of Petroleum Asphaltenes: A Comparison between Mass Spectrometry and Vapor Pressure Osmometry. *Energy Fuels* **2005**, *19* (4), 1548−1560.

(75) Hortal, A. R.; Martínez-Haya, B.; Lobato, M. D.; Pedrosa, J. M.; Lago, S. On the determination of molecular weight distributions of asphaltenes and their aggregates in laser desorption ionization experiments. *J. Mass Spectrom.* **2006**, *41*, 960−968.

(76) Hortal, A. R.; Hurtado, P.; Martínez-Haya, B.; Mullins, O. C. Molecular weight distributions of coal and petroleum asphaltenes from laser desorption ionization experiments. *Energy Fuels* **2007**, *21*, 2863−2868.

(77) Hurtado, P.; Gámez, F.; Martínez-Haya, B. One-step and two-step Ultraviolet and Infrared Laser Desorption Ionization Mass Spectrometry of Asphaltenes. *Energy Fuels* **2010**, *24*, 6067−6073.

(78) Gámez, F.; Hortal, A. R.; Martínez-Haya, B.; Soltwisch, J.; Dreisewerd, K. Ultraviolet laser desorption/ionization mass spectrometry of single-core and multi-core polyaromatic hydrocarbons under variable conditions of collisional cooling: insights into the generation of molecular ions, fragments and oligomers. *J. Mass Spectrom.* **2014**, *49*, 1127−1138.

(79) Mullins, O. C.; Martínez-Haya, B.; Marshall, A. G. Contrasting Perspective on Asphaltene Molecular Weight. This Comment vs the Overview of A. A. Herod, K. D. Bartle, and R. Kandiyoti. *Energy Fuels* **2008**, *22*, 1765−1773.

(80) Pantoja, P. A.; Mendes, M. A.; Nascimento, C. A. O. Contribution of Mass Spectrometry in Assessing Quality of Petroleum Fractions. The Use of Mass Spectrometry for Assessing Asphaltenes. *J. Pet. Sci. Eng.* **2013**, *109*, 198−205.

(81) Rizzi, A.; Cosmina, P.; Flego, C.; Montanari, L.; Seraglia, R.; Traldi, P. Laser Desorption/Ionization Techniques in the Characterization of High Molecular Weight Oil Fractions. Part 1: Asphaltenes. *J. Mass Spectrom.* **2006**, *41* (9), 1232−1241.

(82) Zheng, C.; Zhu, M.; Zhou, W.; Zhang, D. A Preliminary Investigation into the Characterization of Asphaltenes Extracted from an Oil Sand and Two Vacuum Residues from Petroleum Refining Using Nuclear Magnetic Resonance, DEPT, and MALDI-TOF. *J. Energy Resour. Technol.* **2017**, *139* (3), 032905.

(83) Pomerantz, A. E.; Hammond, M. R.; Morrow, A. L.; Mullins, O. C.; Zare, R. N. Asphaltene Molecular-Mass Distribution Determined by Two-Step Laser Mass Spectrometry. *Energy Fuels* **2009**, *23*, 1162−1168.